M344 promotes nonamyloidogenic amyloid precursor protein processing while normalizing Alzheimer's disease genes and improving memory

Claude-Henry Volmar[a,b,1], Hasib Salah-Uddin[a,b], Karolina J. Janczura[a,b,2], Paul Halley[a,b,2], Guerline Lambert[a,b], Andrew Wodrich[a,b], Sivan Manoah[a,b], Nidhi H. Patel[a,b], Gregory C. Sartor[a,b], Neil Mehta[a,b], Nancy T. H. Miles[a,b], Sachi Desse[a,b], David Dorcius[a,b], Michael D. Cameron[c], Shaun P. Brothers[a,b], and Claes Wahlestedt[a,b,1]

[a]Center for Therapeutic Innovation, Miller School of Medicine, University of Miami, Miami, FL 33136; [b]Department of Psychiatry, Miller School of Medicine, University of Miami, Miami, FL 33136; and [c]Department of Molecular Medicine, Scripps Florida, Jupiter, FL 33458

Edited by Li-Huei Tsai, Massachusetts Institute of Technology, Cambridge, MA, and accepted by Editorial Board Member Susan G. Amara September 2, 2017 (received for review May 8, 2017)

Alzheimer's disease (AD) comprises multifactorial ailments for which current therapeutic strategies remain insufficient to broadly address the underlying pathophysiology. Epigenetic gene regulation relies upon multifactorial processes that regulate multiple gene and protein pathways, including those involved in AD. We therefore took an epigenetic approach where a single drug would simultaneously affect the expression of a number of defined AD-related targets. We show that the small-molecule histone deacetylase inhibitor M344 reduces beta-amyloid (Aβ), reduces tau Ser^{396} phosphorylation, and decreases both β-secretase (BACE) and APOEε4 gene expression. M344 increases the expression of AD-relevant genes: BDNF, α-secretase (ADAM10), MINT2, FE65, REST, SIRT1, BIN1, and ABCA7, among others. M344 increases sAPPα and CTFα APP metabolite production, both cleavage products of ADAM10, concordant with increased ADAM10 gene expression. M344 also increases levels of immature APP, supporting an effect on APP trafficking, concurrent with the observed increase in MINT2 and FE65, both shown to increase immature APP in the early secretory pathway. Chronic i.p. treatment of the triple transgenic (APP_{sw}/$PS1_{M146V}$/Tau_{P301L}) mice with M344, at doses as low as 3 mg/kg, significantly prevented cognitive decline evaluated by Y-maze spontaneous alternation, novel object recognition, and Barnes maze spatial memory tests. M344 displays short brain exposure, indicating that brief pulses of daily drug treatment may be sufficient for long-term efficacy. Together, these data show that M344 normalizes several disparate pathogenic pathways related to AD. M344 therefore serves as an example of how a multitargeting compound could be used to address the polygenic nature of multifactorial diseases.

epigenetics | M344 | Alzheimer's | multitarget | APP processing

Alzheimer's disease (AD) is the sixth leading cause of death in the United States and is presently the only top-10 cause of death that has no prevention or effective treatment. With a cost greater than $220 billion for the year 2015 in the United States, AD is a significant burden to the health care system (1). It is expected to reach a prevalence of ∼16 million people in America by the year 2050 (1). Currently approved treatments for AD lack efficacy and are palliative at best. These drugs include cholinesterase inhibitors (donepezil, rivastigmine, and galantamine) or NMDA receptor antagonists (memantine). None of these treatments addresses the molecular pathology present in the brains of AD patients.

AD is confirmed by the diagnosis of dementia associated with the presence of extracellular beta-amyloid (Aβ) plaques in the brain parenchyma and the accumulation of intracellular neurofibrillary tangles—the latter consisting mostly of aggregated hyperphosphorylated tau protein. The accumulation of Aβ results from sequential cleavage of mature (N- and O-glycosylated) amyloid precursor protein (APP) by proteases β- and γ-secretase in the late protein secretory pathway, constituting the amyloidogenic pathway (2, 3). The "amyloid cascade hypothesis" places Aβ at the origin of AD, triggering downstream AD-related events such as tau hyperphosphorylation, neuroplasticity deficits, learning and memory impairments, and, eventually, death (4–9). The accumulation of Aβ can be prevented via the nonamyloidogenic processing of APP by α-secretase cleavage within the Aβ sequence, releasing the neuroprotective metabolite sAPPα and the C-terminal fragment-α (CTF-α, C83). An increase in α-secretase cleavage has been hypothesized as a possible therapeutic target for AD, but currently, due to the difficulties of increasing the activity of an enzyme, most Alzheimer's drug discovery efforts have aimed at three main strategies to reduce Aβ peptide: immunotherapy, inhibition of β-secretase activity, or inhibition of γ-secretase activity. While there are still some single-target drugs in clinical trials, until this date these approaches have been disappointing at treating AD patients (10–14). It is important to note that several other hypotheses have been proposed to explain AD etiology and pathogenesis. Such hypotheses include—but are not limited to—the mitochondrial cascade, the tau, the vascular, and the neuroinflammation hypotheses that, respectively, place decreased mitochondrial activity, hyperphosphorylated-tau pathology, cerebral hypoperfusion, and/or increased inflammatory events (microgliosis,

Significance

Hundreds of failed clinical trials with Alzheimer's disease (AD) patients over the last fifteen years demonstrate that the one-target–one-disease approach is not effective in AD. In silico, structure-based, multitarget drug design approaches to treat multifactorial diseases have not been successful in the context of AD either. Here, we show that M344, an inhibitor of class I and IIB histone deacetylases, affects multiple AD-related genes, including those related to both early- and late-onset AD. We also show that M344 improves memory in the 3xTg AD mouse model. This work endorses a shift to a multitargeted approach to the treatment of AD, supporting the therapeutic potential of a single small molecule with an epigenetic mechanism of action.

Author contributions: C.-H.V., H.S.-U., K.J.J., P.H., and C.W. designed research; C.-H.V., H.S.-U., K.J.J., P.H., G.L., A.W., S.M., N.H.P., G.C.S., N.M., N.T.H.M., S.D., D.D., and M.D.C. performed research; C.-H.V., H.S.-U., K.J.J., P.H., G.L., A.W., S.M., N.H.P., G.C.S., N.M., M.D.C., S.P.B., and C.W. analyzed data; C.-H.V. and C.W. wrote the paper; C.-H.V., H.S.-U., P.H., and C.W. conceived of the project; and S.P.B. and C.W. provided financial support.

The authors declare no conflict of interest.

This article is a PNAS Direct Submission. L.-H.T. is a guest editor invited by the Editorial Board.

Freely available online through the PNAS open access option.

[1]To whom correspondence may be addressed. Email: CVolmar@med.miami.edu or cwahlestedt@med.miami.edu.

[2]K.J.J. and P.H. contributed equally to this work.

This article contains supporting information online at www.pnas.org/lookup/suppl/doi:10.1073/pnas.1707544114/-/DCSupplemental.

astrogliosis, and proinflammatory cytokines) as root causes of AD (15–19).

Several AD susceptibility genes, identified in patients through linkage and genome-wide association studies, suggest that AD is a complex polygenic disease (5, 20–23). Due to the polygenicity of AD and the vast number of failures with the single-target approach, many have hypothesized that it will be necessary to utilize combination therapies, and/or treatment at preclinical or prodromal stages for this disease. Here, we tested this hypothesis with an epigenetic approach where we hypothesized a single small molecule could simultaneously affect the expression of many AD-related drug targets, thus bypassing the need for drug combinations. Moreover, since gene expression changes through the remodeling of chromatin play an important role in memory formation (24–27), and epigenetic changes are widely reported in AD brain (28–31), such an epigenetic-directed compound could also prevent memory decline in an AD mouse model.

We provide data describing that the histone deacetylase inhibitor (HDACi) M344 {4-(diethylamino)-*N*-[7-(hydroxyamino)-7-oxoheptyl]benzamide} modifies several of the AD-related pathways and thus holds some therapeutic potential. M344 was first synthesized in 1999 by Jung et al. (32) and, while little studied compared with many other HDACis, it was reported to significantly increase survival motor neuron 2 (*SMN2*) gene expression—a gene associated with the severity of proximal spinal muscular atrophy, an orphan disease (33, 34). In the experiments described below we show that M344 favorably addresses a number of key genes reported to be involved in early- and late-onset AD pathogenesis and attenuates cognitive decline in a chronically treated AD mouse model.

Results

Compound Selectivity Profile. Since little is known about the HDAC selectivity profile of M344 (32), we tested its potency at inhibiting all 11 known zinc-dependent HDACs. The half-maximal inhibition (IC_{50}) concentration of M344 was calculated for each HDAC with a ten-point concentration response curve in duplicates, using titration of 1:3 dilutions (BPS Bioscience). Each HDAC was also inhibited by an appropriate positive control, such as vorinostat (suberoylanilide hydroxamic acid, SAHA) or trichostatic acid (TSA). The HDAC activity profile revealed that M344 showed potent activity for class I (HDACs 1, 2, 3, and 8) and IIB (HDACs 6 and 10) in the submicromolar to the micromolar range (Table1), suggesting selectivity for these classes. Detailed concentration curves are provided in Fig. S1.

Table 1. M344 HDAC selectivity profile

	IC_{50}, μM	
HDACs	M344	Reference
HDAC1	0.048	0.083 (SAHA)
HDAC2	0.12	0.19 (SAHA)
HDAC3	0.032	0.046 (SAHA)
HDAC4	26.80	2.21 (TSA)
HDAC5	15.82	1.18 (TSA)
HDAC6	0.0095	0.027 (SAHA)
HDAC7	17.09	1.34 (TSA)
HDAC8	1.34	0.61 (TSA)
HDAC9	48.80	5.20 (TSA)
HDAC10	0.061	0.089 (SAHA)
HDAC11	>100 μM 18% at 100 μM	27 (TSA)

Summary of half-maximal inhibitory concentration in biochemical activity assay for each zinc-dependent HDAC. Each sample was tested in duplicate, with a 10-point dose–response of one to three dilutions, starting at 100 μM. M344 shows greater potency at inhibiting classes I and IIB HDACs.

Effects of M344 on AD-Related Genes. Using NanoString nCounter technology (35, 36), we investigated the effects of M344 on 71 AD-related genes after 48 h treatment of HEK cells overexpressing the familial APP Swedish double mutation (KM670/671NL) (5)—HEK/APP_{sw}—a well-characterized AD cell model (6, 37, 38). The heat map generated from this experiment illustrates the differential expression of genes after M344 treatment. With a false discovery rate (FDR) less than 5%, several AD-related and neuroplasticity genes are significantly up- and down-regulated by M344 (Fig. 1 and Table S1). Interestingly, several genes reported to be neuroprotective when up-regulated in AD are increased by M344 treatment. Among these genes with increased expression are brain-derived neurotrophic factor (BDNF) (3.4-fold, $P < 0.0001$), neuregulin (NRG1) (4.8-fold, $P < 0.0001$), NAD-dependent deacetylase sirtuin-1 (SIRT1) (1.6-fold, $P < 0.0001$), a disintegrin and metalloprotease 10 (ADAM10) (1.40-fold, $P < 0.0001$), ADAM19 (1.5-fold, $P < 0.01$), and repression element-1 silencing transcription factor (REST) (1.2-fold, $P < 0.0001$). Of particular interest are the ADAM family members and SIRT1, which promote nonamyloidogenic APP processing thought to be beneficial in both early- and late-onset AD.

A similar trend toward nonamyloidogenic processing and anti-AD protection is also observed in significantly down-regulated genes depicted in the NanoString nCounter heat map. Among them are glycogen synthase kinase 3-β (GSK3β) (−1.4-fold, $P < 0.0001$), Nicastrin (NCSTN) (−3.2-fold, $P < 0.0001$), anterior pharynx-defective 1 (APH1) (−1.8-fold, $P < 0.0001$), β-site APP-Cleavage Enzyme 1 (BACE1) (−1.7-fold, $P < 0.0001$), BACE2 (−3.2-fold, $P < 0.0001$), cluster of differentiation 40 ligand (CD40L) (−1.5-fold, $P < 0.01$), and C-X-C Motif Chemokine Receptor 2 (CXCR2) (−2.0-fold, $P < 0.0001$), which are all genes hypothesized to counter AD phenotype and pathogenesis (37, 39–41). In the case of late-onset AD (LOAD) genes, apolipoprotein-E-ε4 (APOEε4) is reduced (−1.8-fold, $P < 0.0001$), which may be therapeutically beneficial (21, 42). There is also a significant increase observed with the bridging integrator 1 (BIN1) (2.2-fold, $P < 0.0001$)—reported to increase tau pathology and BACE1-dependent processing of APP (43, 44). Adenosine triphosphate-binding cassette subfamily A member 7 (ABCA7) is also up-regulated (2.1-fold, $P < 0.0001$), which is thought to be protective. ABCA7 loss of function is a risk factor for LOAD, and deficiency in ABCA7 increases production of Aβ (45, 46). Several Alzheimer's-related genes tested such as complement receptor 1 (CR1), interleukin 10 (IL10), cluster of differentiation 33 (CD33) and APOE-ε2 showed no change in gene expression by M344, showing that this molecule does not randomly affect all genes.

M344 Effects on α- and β-Secretases and APP Processing. With the observation of significant increases in several α-secretases and decreases in β-secretases in the NanoString experiments we confirmed the effect of M344 on ADAM10 and BACE1 (the two predominant α- and β- secretases involved in brain APP processing) using real-time (RT) qPCR and Western blotting (Fig. 2). Treatment of HEK/APP_{sw} cells with 10 μM of M344—a concentration that will inhibit target HDACs (Table 1), and which we show displays no toxicity (Fig. 3)—resulted in significant increase in ADAM10 gene expression (1.80-fold, $P < 0.0001$) and protein levels (121.0%, $P < 0.001$), similar to results obtained with the NanoString. BACE1 gene expression (−3.6-fold, $P < 0.0001$) and protein level (−58.1%, $P < 0.0001$) also were confirmed to decrease after treatment of HEK/APP_{sw} cells with M344, replicating the NanoString results (Fig. 2).

Because we observed significant regulation of several APP-cleaving secretases after treatment of HEK/APP_{sw} cells with M344, we hypothesized that there will be an increase in full-length APP (holo-APP) in the presence of M344. Unexpectedly,

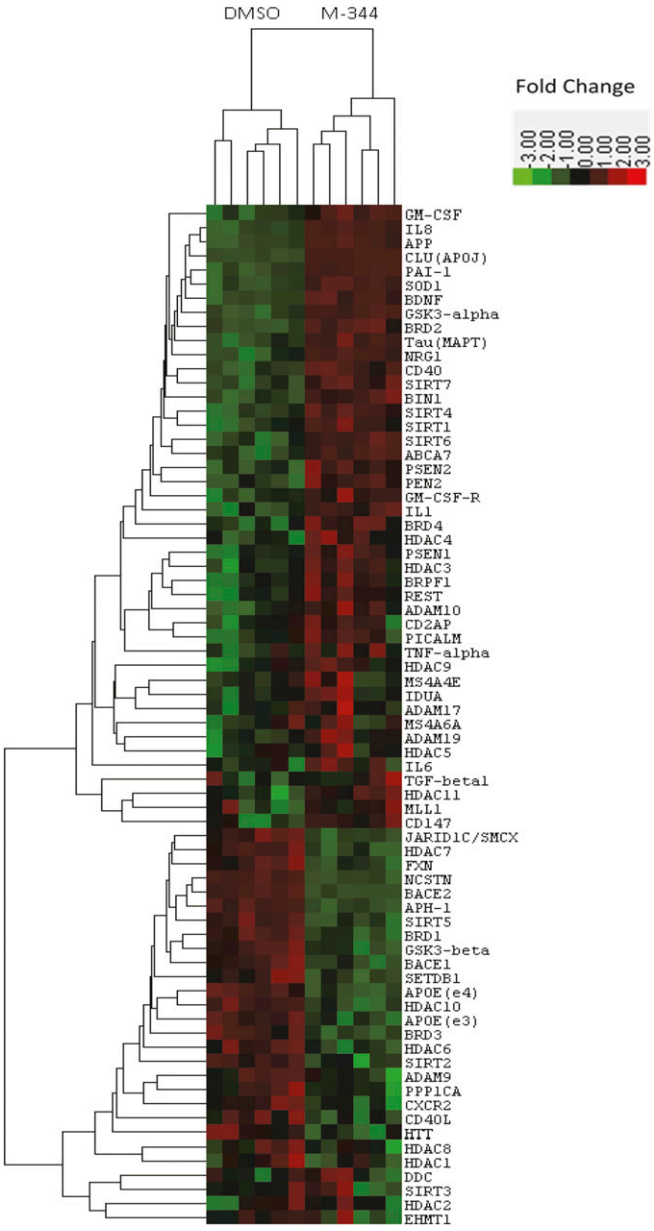

Fig. 1. Heat map summarizing up- and down-regulation of genes after M344 treatment of HEK/APP_{sw} cells. Green indicates down-regulation of gene expression. Red indicates up-regulation. Changes are considered significant if FDR < 0.05, $P < 0.05$, and fold change > 1.2. $n = 6$. NanoString Data were analyzed using nSolver software 3.0.

we observed a significant increase (361.9%, $P < 0.0001$) of immature APP after treatment with M344 (Fig. 2). We also investigated the levels of sAPPα and CTF-α, two APP metabolites that result from α-secretase cleavage of APP, and observed significant increases (118.0%, $P < 0.0001$ for sAPPα and 35.9% for CTF-α, $P < 0.05$), functionally supporting the increase of α-secretases and decrease in β-secretase observed in the NanoString, RT-qPCR, and with Western blots. As an additional control, we used garcinol, a histone acetyl transferase (HAT) inhibitor of p300 and PCAF (47), hypothesizing that a HAT inhibitor would cause opposite effects from those observed with M344. Garcinol caused significant increases in both mature APP (37.9%, $P < 0.01$) and BACE1 (54.3%, $P < 0.0001$), whereas M344 treatment resulted in significant decreases in these APP processing parameters, as described above. Moreover, garcinol treatment caused sAPPα to significantly decrease (−33.6%, $P < 0.01$) compared with a significant increase of 118% observed with M344, further supporting a histone acetylation-dependent mechanism. We also show, in these cells, that M344 significantly increases acetylation of H3K27 (245.3%, $P < 0.01$) and H4K12 (95.5%, $P < 0.05$) after 48 h of treatment (Fig. S2). We also show a time-dependent increase of both pan-lysine and H4K12 acetylation (Fig. S3). We further support an HDAC-dependent effect by shRNA silencing of class I and IIb HDACs—targets of M344—and show significant increases in CTFα, ADAM10, and holo-APP protein levels with silenced HDACs 1, 2, 3, and 6 (Fig. S4).

Effects of M344 on Aβ Accumulation. Since there was a shift toward nonamyloidogenic processing, we hypothesized that Aβ level would decrease in the presence of M344. We indeed observed a significant decrease of Aβ in HEK/APP_{sw} cells treated with 10 μM of M344. To further validate an HDAC mechanism we tested several other HDAC inhibitors that also significantly reduced $Aβ_{1–42}/Aβ_{1–40}$ accumulation in these cells (Fig. 3*A*). We then verified that these effects were caused by an effect on Aβ accumulation and not due to cytotoxicity by performing a cell viability assay (CellTiter-Glo; Promega) on treated cells versus controls (Fig. 3*B*). The cell viability results demonstrate that cells treated with M344 showed no cell death and that M344 appears to be less toxic than the other HDAC inhibitors tested.

Effects of M344 on APP Trafficking Genes. Considering immature APP (N-glycosylated) is significantly increased with M344 treatment (Fig. 2 and Fig. S5), and with the knowledge that immature APP localizes mostly to the early protein secretory pathway, then matures upon trafficking to the late secretory pathway where it is cleaved by β-secretase, we hypothesized that M344 affects gene expression of proteins involved in APP trafficking. MINT2 (APBA2, X11L) and FE65 (APBB1) expressions are two important regulators of APP endocytosis shown to increase immature APP in the early secretory pathway, subsequently preventing APP interaction with BACE in the late endosome (2, 48). Interestingly, we observed significant increases of both MINT2 (2.7-fold, $P < 0.01$) and FE65 (1.7-fold, $P < 0.05$) gene expression in HEK/APP_{sw} cells treated with M344 (Fig. 4 *A* and *B*). These data further support the anti-AD profile of M344 because increased MINT2 or FE65 has been linked to decreased Aβ production and less amyloid deposition in APP transgenic mice brain (49, 50).

M344 Effects on Neuroprotective Genes BDNF and REST. Treatment of HEK/APP_{sw} cells for 48 h revealed significant increases of both BDNF (7.1-fold, $P < 0.0001$) and REST (4.2-fold, $P < 0.001$) gene expression (Fig. 4 *C* and *D*) and of BDNF protein expression (42.3%, $P < 0.01$) (Fig. 4*E*). Due to lack of a reliable REST antibody we were unable to determine REST protein levels. M344 also increased REST gene expression in control HEK-293 cells, although to a lesser extent compared with HEK/APPsw (1.2-fold, $P < 0.05$) (Fig. 4*D*). Fig. 4*D* also shows that the presence of APP_{sw} in the cells significantly reduced REST expression (−2.0-fold, $P < 0.05$), reminiscent of the human condition reported in AD patients (51).

M344 Is Brain-Penetrant and Increases Histone Acetylation in Vivo. We conducted pharmacokinetic studies with 10 mg/kg of M344 injected i.p. Fig. 5 *A* and *B* show that M344 concentrations peak rapidly at 15 min in both plasma and the brain. Of note, M344 reaches brain concentrations of 47 ng/mL ($P < 0.05$), a value equivalent to 0.13 μM that is sufficient to inhibit HDACs 1, 2, 3, 6, and 10 as shown in Table 1 and Fig. S1. Fig. 5 *C–E* show that M344 significantly increases acetylation of histone H4K12 in the frontal cortex, but not in the cerebellum. Fig. 5*F* shows that

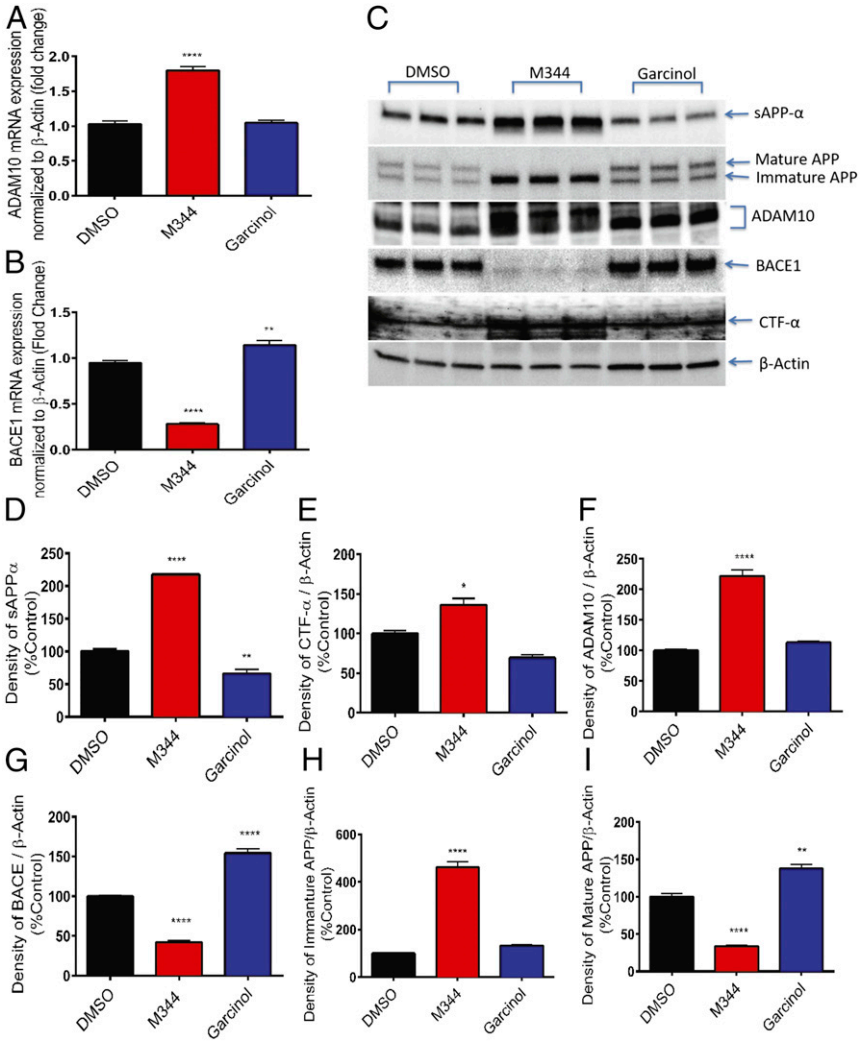

Fig. 2. Effects of M344 on ADAM10, BACE1, and APP processing in HEK/APP_{sw} cells. (*A*) RT-qPCR data showing significant increase of ADAM10 and (*B*) significant decrease of BACE1 after M344 treatment. (*C*) Representative Western blots of APP metabolites ADAM10 and BACE1 after M344 and garcinol treatments. Densitometry of bands from Western blots show significant increases in (*D*) sAPPα and (*E*) CTFα after M344 treatment. (*F*) There is a significant increase in the ADAM10 98kDa precursor compared with DMSO controls and (*G*) a significant decrease in BACE1 expression with M344. (*H*) M344 significantly increases immature APP and (*I*) decreases mature APP. All cells were treated with either 0.2% DMSO buffer or 10 μM of compounds in 0.2% DMSO. $*P < 0.05$, $**P < 0.01$, $****P < 0.0001$; $n = 3$; mean ± SEM.

after 15 min of 10 mg/kg i.p. injection there is ∼1.4% brain/plasma ratio with 3.1 ± 0.71 μM free concentration and 0.39 ± 0.04 free fraction of M344 in plasma.

Effects of M344 on Y-Maze Spontaneous Alternation in 3xTg APP_{sw}/$PS1_{M146V}$/Tau_{P301L} Mice. We then tested M344 in the 3xTg AD mice overexpressing APP_{sw}, Tau_{P301L}, and Presenilin 1 (PS1, PSEN1) (52) using a battery of behavioral tests. In 3xTg AD mice that were repeatedly i.p. treated with M344 (for ∼4 mo, as described in *Materials and Methods*) we observed a dose-dependent increase in Y-maze spontaneous alternation (3 mg/kg, 67.0%, $P < 0.05$; 10 mg/kg, 71.2%, $P < 0.01$) compared with vehicle controls (Fig. 6*A*). No difference in total number of arm entries was observed (Fig. 6*B*), demonstrating no deficits in motor function and supporting that the increased spontaneous alternation observed in treated mice is due to increased spatial memory and willingness to explore new environments.

Effect of M344 on Open Field Behavior and Novel Object Recognition. We further tested the effects of M344 on locomotor behavior using the open field test. No significant difference was observed between M344-treated animals and controls for distance traveled or velocity (Fig. 6 *C* and *D*). Having observed no difference in locomotor behavior in the treated and control mice, we proceeded to test for novel object recognition in the same open field arena. In this test, at both 3 mg/kg and 10 mg/kg doses, treated mice significantly outperformed control mice in novel object exploration duration (3 mg/kg: 66.5%, $P < 0.05$; 10 mg/kg: 57.2%, $P < 0.05$) (Fig. 6*E*) and novel object exploration frequency (3 mg/kg: 47.8%, $P < 0.05$; 10 mg/kg: 47.3%, $P < 0.05$) (Fig. 6*F*).

Effects of M344 on Barnes Maze Performance. We further evaluated spatial memory in the 3xTg AD mice treated with 3 mg/kg and 10 mg/kg of M344 using a Barnes maze. We observed significantly fewer errors in acquisition trials 3 and 5 for mice that received 10 mg/kg of M344 ($P < 0.05$) and fewer errors in trial 5 for those treated with 3 mg/kg ($P < 0.05$) compared with vehicle-treated controls (Fig. 6*G*). After 24 h of rest, in the probe trial both mice treated with M344 committed fewer errors than controls (3 mg/kg: −44.6%, $P < 0.05$; 10 mg/kg: −53.8%, $P < 0.01$) (Fig. 6*H*), indicating increased spatial memory in these mice.

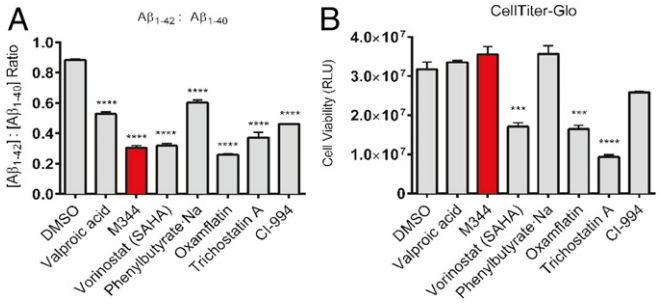

Fig. 3. Effects of different HDAC inhibitors on Aβ42/Aβ40 ratio and cell viability. (*A*) Several HDAC inhibitors significantly reduce Aβ42/Aβ40 ratio at 10 μM concentration. (*B*) M344 presents no effect on cell viability, whereas SAHA, oxamflatin, and trichostatin significantly reduce cell viability. All drugs were tested in duplicates. Mean ± SEM; ***$P < 0.001$, ****$P < 0.0001$.

Effects of M344 on AD-Like Pathology in the Hippocampus of 3xTg AD Mice. M344 significantly decreased $A\beta_{1-42}$ in the hippocampus of mice treated with doses of 3 mg/kg (−42.7%, $P < 0.05$) and 10 mg/kg (−35.6%, $P < 0.05$) (Fig. 7*A*). M344 significantly increased ADAM10 gene expression only in the hippocampus of mice treated with 10 mg/kg (2.1-fold, $P < 0.05$) (Fig. 7*B*). Only treatment with 3 mg/kg of M344 resulted in a significant decrease of BACE1 gene expression (−1.8-fold, $P < 0.05$) (Fig. 7*C*). We also observed significant decrease in phosphorylation of tau at Ser^{396}—a residue found in paired helical filaments in brain neurofibrillary tangles of AD patients—at both 3 mg/kg (−58.2%, $P < 0.01$) and 10 mg/kg (−57.7%, $P < 0.01$) (Fig. 7*D*).

Discussion

We show that the HDAC inhibitor M344 is a potent inhibitor of class I and class IIB HDACs that simultaneously regulates the expression of several high-priority genes related to EOAD, LOAD, synaptic plasticity, and neuroprotection in the HEK/APP_{sw} cell model (Table 1, Fig. 1, and Fig. S1). In support of the gene expression data, we show that M344 significantly reduces $A\beta_{1-42}/A\beta_{1-40}$ ratio with no negative effects on cell viability, while also appearing to have a better in vitro toxicity profile than other HDAC inhibitors tested (Figs. 1–3). A mechanism that can explain this decrease in $A\beta_{1-42}/A\beta_{1-40}$ ratio is the M344-induced down-regulation of γ-secretase complex components NCSTN and APH1 (Fig. 1), which would reduce APP cleavage at the relevant sites. However, down-regulating the γ-secretase complex—comprising PSEN1 or PSEN2, PEN2, NCSTN, and APH1—is troublesome since γ-secretase also cleaves NOTCH, a transmembrane protein whose cleavage products are reported to promote neurogenesis. Inhibition of NOTCH processing has been cited as a possible cause of the recent γ-secretase inhibitor clinical trial failures (12–14). Although both NCSTN and APH1 are significantly down-regulated with M344, we would not expect a decrease in the processing of NOTCH since M344 also increases other components of the complex in PEN2, PSEN1, and PSEN2 (Fig. 1), which have been demonstrated to be sufficient for γ-secretase–dependent NOTCH processing (53). The decrease in $A\beta_{1-42}/A\beta_{1-40}$ ratio could also be the result of a combined effect of decreasing the expression of CXCR2, NCSTN, and APH1. Depletion of CXCR2 has been reported to reduce γ-secretase cleavage of APP (40). The effect of M344 or other HDACs on CXCR2-mediated γ-secretase APP processing is not known and deserves further investigation. Because we only observed significant reduction of $A\beta_{1-42}/A\beta_{1-40}$ ratio in cells silenced for HDAC3 (Fig. S4*F*), it may be worth investigating the effects of HDAC3 function on CXCR2 and γ-secretase components.

In cases of EOAD involving APP mutations such as APP_{sw}, the overproduction of Aβ is often due to excess cleavage by β-secretases (6). Here, we show that compound M344 significantly reduces β-secretases BACE1 and BACE2, concurrent with observed decreases in the accumulation of $A\beta_{1-42}$ (Figs. 2, 3, and 7), indicating that HDAC inhibition is an alternative approach to BACE1 inhibition. Of note, a BACE1 inhibitor, verubecestat (MK-8931), recently failed in phase III trials (10). Thus, an epigenetic compound that is able to reduce BACE1-mediated metabolites as one of its targets in the AD network represents a novel way to regulate BACE activity, which has been challenging (54).

The up-regulation of α-secretase has been proposed as a highly desirable therapeutic target for AD. Here, we report that the M344 compound also significantly increases the gene expression of α-secretases ADAM10 and ADAM19, concurrent with the observed increases in the metabolites sAPPα and CTFα after M344 treatment (Fig. 2 and Fig. S6). Similar effects have been reported with the HDAC inhibitor apicidin up-regulating the expression of ADAM10 via an HDAC2/3 mechanism involving the transcription factor USF-1 (55). Here we show in

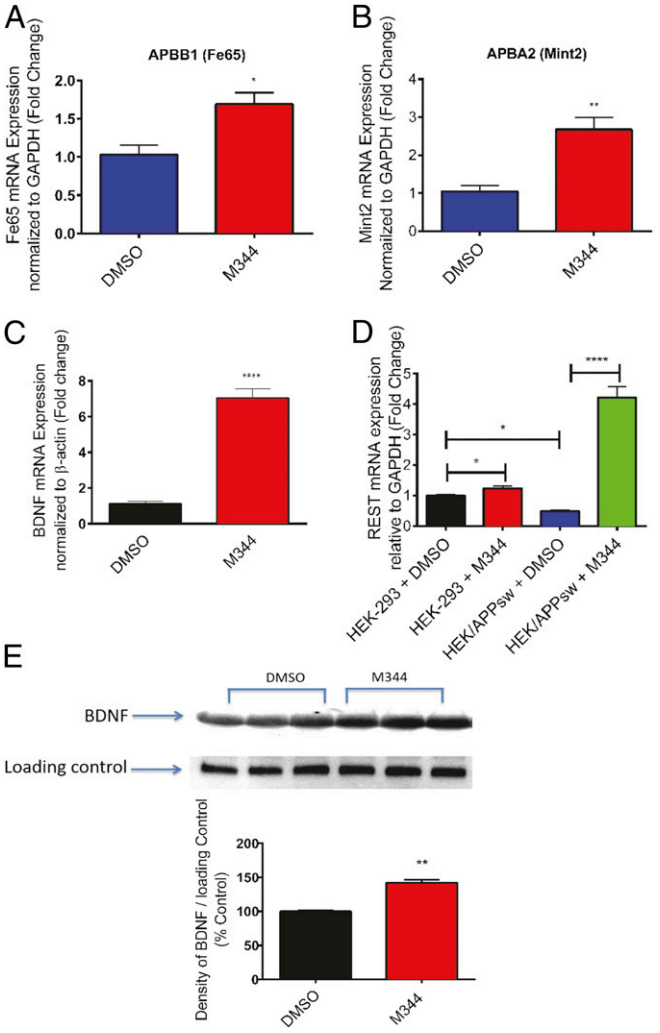

Fig. 4. Gene expression levels of APP trafficking and neuroprotective genes after M344 treatment of HEK/APP_{sw} cells. Treatment with 10 μM of M344 causes a significant increase in (*A*) FE65 and (*B*) MINT2. (*C*) RT-qPCR results show BDNF gene expression is significantly increased in the presence of 10 μM M344. (*D*) RT-qPCR data show that the overexpression of APP_{sw} decreases REST levels below baseline, comparing HEK + DMSO versus HEK/APP_{sw} + DMSO. Compound M344 significantly increases REST gene expression in HEK-293 cells and in HEK/APPsw cells. (*E*) Western blot showing that M344 significantly increases BDNF protein level. $n = 3–6$; mean ± SEM; *$P < 0.05$, **$P < 0.01$, ****$P < 0.0001$.

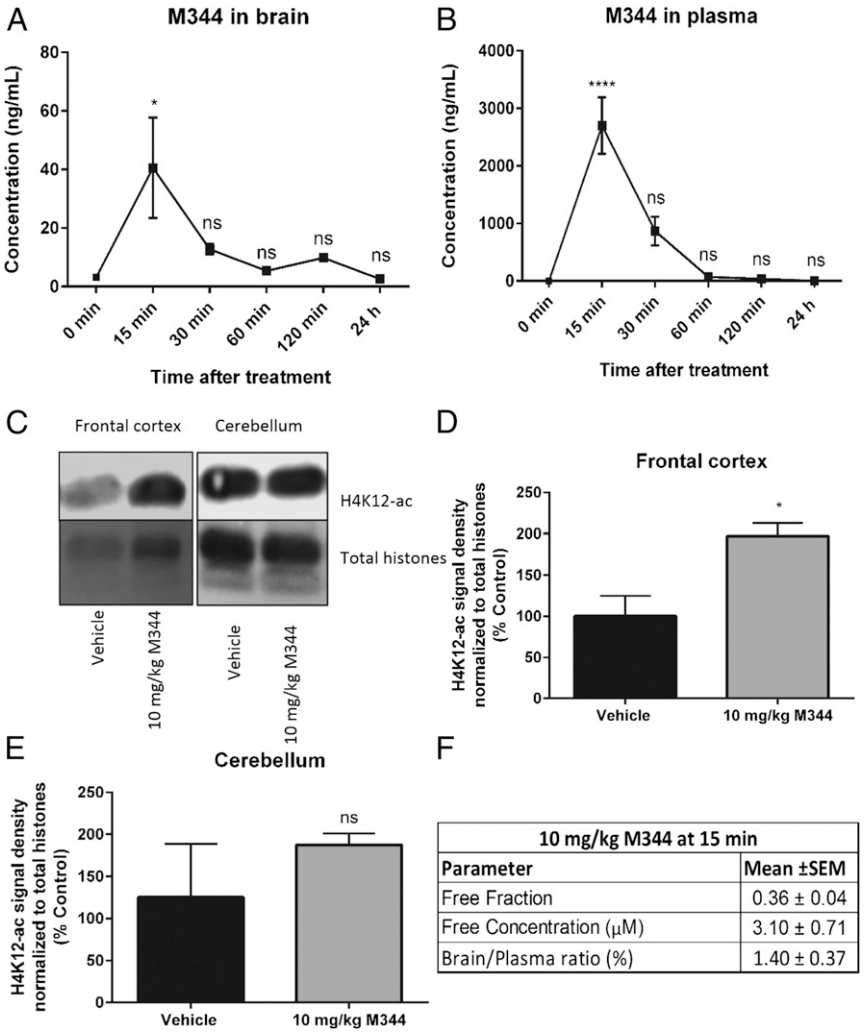

Fig. 5. Pharmacokinetics and histone acetylation after M344 treatment of wild-type mice. (*A*) I.p. injection of 10 mg/kg of M344 results in significant increase of M344 brain concentration after 15 min of treatment. (*B*) The same treatment also causes significant increase of M344 plasma concentrations after 15 min. (*C*) Representative Western blots from purified histone extracts show increased acetylation of H4K12 in the frontal cortex but not in the cerebellum after i.p. injection with 10 mg/kg of M344 for 30 min. (*D*) Quantification of frontal cortex Western blots from purified histone extracts shows significant increase in H4K12 acetylation after M344 treatment. (*E*) Quantification of cerebellum Western blots shows there is no significant difference in acetylation at the H4K12 residue in purified histone extracts from the cerebellum after M344 treatment. (*F*) Summary of M344 free fraction, free concentration, and brain/plasma ratio levels after 10 mg/kg i.p. treatment. $n = 3$; mean ± SEM; $^{*}P < 0.05$, $^{****}P < 0.0001$. ns, not significant.

HEK/APP$_{sw}$ cells that it is possible that the effect on ADAM10 is mediated by HDACs 1, 2, 3, and 6 because M344 inhibits these HDACs, and silencing experiments caused increased protein levels of ADAM10 and CTFα (Fig. S4 *A* and *B*). We also observe a significant increase in SIRT1 expression, which has been shown to promote ADAM10 cleavage of APP (56). Thus, it is also possible that the increased nonamyloidogenic processing induced by M344 is partially a SIRT-1-mediated effect, making M344 an HDAC inhibitor affecting both zinc-dependent and class III NAD-dependent HDACs.

We also observed, in HEK/APP$_{sw}$ cells, significant increases in the APP trafficking genes MINT2 and FE65, and of the neuroprotective genes BDNF, NRG1, and REST, all genes reported to be beneficial against AD if up-regulated (Fig. 4). Increased REST expression correlates with healthy aging, cognitive preservation, and longevity (51). Our findings support studies by others that have shown that the HDAC inhibitor SAHA and inhibition of HDACs 2 and 3 increase BDNF gene expression (57, 58). Further, large concentrations—0.8–5 mM—of β-hydroxybutyrate increase BDNF expression via inhibition of HDACs 2 and 3 (59). Since M344 inhibits these two HDACs, M344-mediated induction of BDNF expression (Fig. 4 *C* and *E* and Fig. S7) is likely due to activity on HDACs 2 and 3. To our knowledge, inhibition of class I and IIb HDACs has not previously been shown to increase the expression of APP trafficking genes MINT2 and FE65 involved in decreased APP cleavage.

Among LOAD-related genes, M344 decreases the expression of APOEε4—for which the presence of just one ε4 allele represents the greatest risk factor of developing AD (21, 42). M344 also increases the expression of BIN1—the second-greatest reported LOAD risk factor (43, 44). Effects of M344 at both genes would be expected to be protective. Increased APOEε4 also elevates Aβ accumulation (60). Decreased BIN1 has been reported to promote tau pathology (43). Similarly, M344 also up-regulates other LOAD risk-factor genes (i.e., ABCA7 and PICALM) whose deficiencies have been shown to promote AD pathology (43–46, 61). M344 also shows significant decrease of CD40L, the cognate ligand of CD40, which has been proposed as a diagnostic biomarker in LOAD (62), and whose signaling has been reported to increase Aβ-induced microglial

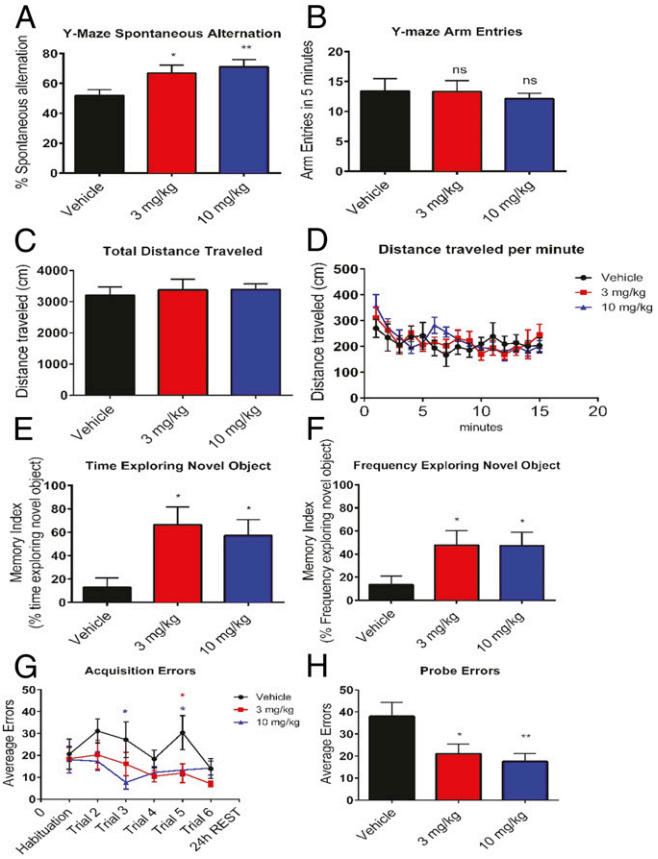

Fig. 6. Effects of M344 treatment on behavior of the 3xTg AD mice. (*A*) I.p. injection of M344 increases Y-maze spontaneous alternation in mice at both 3 mg/kg and 10 mg/kg, with (*B*) showing no significant differences in total arm entries. (*C*) Open field test shows that animals treated with M344 have no locomotion deficits and (*D*) travel at similar velocity compared with controls. (*E*) Injection of 3 mg/kg and 10 mg/kg of M344 increases novel object recognition performance of mice as determined by duration of exploration and (*F*) frequency of novel object exploration. (*G*) Barnes maze acquisition trials for these mice show significantly fewer errors in trial 3 for mice treated with 10 mg/kg of M344 and in trial 5 for mice treated with 3 mg/kg or 10 mg/kg. (*H*) Barnes maze probe trial shows that M344 significantly increases spatial memory as determined by decreased errors in treated mice. Vehicle: $n = 10$; 3 mg/kg: $n = 9$; 10 mg/kg: $n = 8$; mean ± SEM; $^{*}P < 0.05$, $^{**}P < 0.01$. ns, not significant.

activation and plaque-associated tau phosphorylation in AD mice (39, 63). The M344-mediated reduction in CD40L likely results in interruption of CD40-CD40L interaction. Such a disruption of CD40–CD40L signaling has been shown to be beneficial in reducing AD-like pathogenesis and increase cognition in AD mice (37, 39, 64).

We show that i.p. treatment of mice with 10 mg/kg of M344 causes a maximum plasma concentration of ∼8.8 μM (C_{max}) and gets into the brain with a peak of about 0.13 μM (C_{max}) after 15 min of treatment. That concentration is high enough to reach the IC_{50} values of HDAC1 (0.048 μM), HDAC2 (0.12 μM), HDAC3 (0.032 μM), HDAC6 (0.0095 μM), and HDAC 10 (0.061 μM) but not HDAC8 (1.34 μM). With a low molecular weight (307.4), a LogP of ∼1.06, as well as high free fraction and free concentration levels in plasma (Fig. 5*F*), M344 has the properties of a brain-penetrant compound. The fact that brain plasma ratio ranges from 1.4% at 15 min to 1.7% at 30 min suggests quick removal by brain Pgp and Bcrp efflux transporters, similar to what is observed with SAHA, a related compound (65). Despite its high rate of removal in the brain, M344 causes significant increases of H4K12 acetylation in the cortex of mice, but not in the cerebellum (Fig. 5). Deregulation of H4K12 acetylation is linked to cognitive impairment associated with aging, and increased acetylation at that mark may rescue memory (66, 67). Our data with the 3xTg mice indicate that one dose per day of M344 at 3 mg/kg or 10 mg/kg for 4 mo is enough to trigger an anti-AD profile without observable adverse effects. It is plausible that over the course of 4 mo the relatively low C_{max} is the reason no toxicity is observed with M344 treatment.

We show that treatment of the well-established 3xTg AD mouse model with doses as low as 3 mg/kg of M344 results in improvement of learning and memory in different behavioral tests, with no effects on locomotor activity (Fig. 6). Indeed, we observed significant increases in Y-maze spontaneous alternation, a measure of hippocampus-dependent spatial memory and the willingness of mice to explore new environments (68, 69). We also observed superior performance of the 3xTg AD mice treated with M344 in both the novel object recognition test and the probe test of the Barnes maze—a spatial memory test similar to the Morris water maze. Interestingly, Tg2576 AD mice treated with 25 mg/kg and 50 mg/kg of SAHA (also known as vorinostat), a compound closely related to M344, has shown positive effects on synaptic plasticity at the long-term potentiation level, but not behaviorally in the fear conditioning paradigm (65). Such a discrepancy with our study could be due to the different tests used, the animal model, age of animals, and length of treatment. In a different animal model (aged APP/PS1 mice), Kilgore et al. (70) saw improvement of cognitive behavior with i.p. injections of 50 mg/kg of SAHA, supporting an HDAC class I inhibition approach in their paper. Another study using SAHA administered 2 mg/d orally to aged (10-mo-old) APP-PS1-21 AD mice observed partial improvement of spatial memory, reduction of transcriptional inflammatory response, and increased H4K12 acetylation, with no significant differences observed in Aβ plaques (66). Although they used different animals and paradigms, focusing more

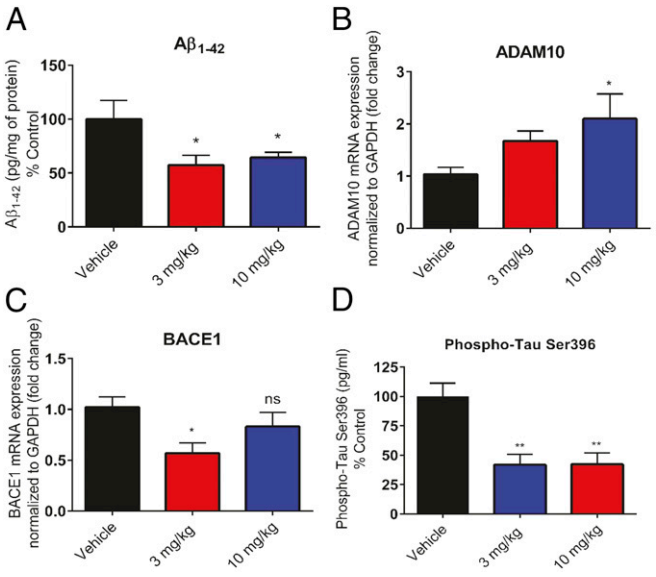

Fig. 7. Analysis of $A\beta_{1-42}$, BACE1, ADAM10, and phospho-tau Ser^{396} in the hippocampus of 3xTg AD mice. (*A*) M344 significantly reduces levels of $A\beta_{1-42}$ at 3 mg/kg, as determined by ELISA. (*B*) RT-qPCR results show that ADAM10 gene expression is significantly increased in the hippocampus of 3xTg mice treated with 10 mg/kg. (*C*) BACE1 mRNA level is significantly reduced in the hippocampus of mice treated at 3 mg/kg. (*D*) Both 3 mg/kg and 10 mg/kg of M344 significantly decrease tau phosphorylation at serine residue 396, as determined by ELISA. Mean ± SEM; $^{*}P < 0.05$, $^{**}P < 0.01$. ns, not significant.

on aging and the transcriptome, the Kilgore et al. (70) and the Benito et al. (66) studies both support our findings that targeting several HDACs with a small-molecule inhibitor provides a multifactorial approach to normalize AD-related genes. The lack of difference in Aβ levels observed in Benito et al. (66) is likely due to three main differences between the studies: (*i*) the length of treatment (4 wk versus 4 mo in our case), (*ii*) the stage of AD-like symptoms of the animals at the start of treatment (postdisease state versus presymptomatic), and (*iii*) the Aβ measurement technique (immunohistochemistry versus ELISA). Overall, the two studies are concordant. Other studies with HDACis such as 200 mg/kg sodium 4-phenylbutyrate in Tg2576 AD mice (71) or 50 mg/kg of the class II mercaptoacetamide compound W2 in 3xTg AD mice (72) also show positive effects on memory, further suggesting feasibility of the approach. However, somewhat in contrast, treatment of 3xTg AD mice with even low dose of M344 significantly decreases levels of the molecular targets BACE1, $A\beta_{1-42}$, and phospho-tau Ser^{396} in the hippocampus. Separate studies have reported other HDACis to be beneficial for AD, either due to induced increase in BDNF gene expression, or decrease in GSK3β expression, or decrease in tau phosphorylation, or decrease in Aβ accumulation to increase cognition in AD mouse models (31, 70, 73–77). Here, we propose that such effects are due to the multitarget nature of these HDAC inhibitors, similarly to M344, and not to a single target.

It is important to emphasize that most of the work performed with HDACis on AD models in the literature has been conducted on old animals, after AD-like disease onset. This approach has yielded poor results in AD patients. Many clinical trial failures have been on old patients with mild to moderate disease, and reversing the pathology may not readily result in alleviation of symptoms. As the field is moving toward trials on preclinical/prodromal AD populations (10), we opted to start treatment of mice before the development of disease. Since 3xTg mice have been reported to present overt molecular and behavioral AD-like pathology at the age of 6 mo, we started treatment of 3-mo-old presymptomatic 3xTg mice 5 d a week for about 4 mo to evaluate the possibility of low doses of this drug as a preventive measure for AD. This method was successful at preventing AD-like pathogenesis at molecular and behavioral levels. This study does not, however, show whether M344 would continue to be beneficial for longer-term studies (i.e., beyond 7 mo of age when AD-like symptoms are more severe). Other limitations of the work presented here include the possibility of HDACis increasing the acetylation of proteins other than histones, such as tau acetylation reported to be a promoter of tau pathology (78, 79). We have, for instance, shown that treatment of HEK/APP_{sw} cells with M344 results in an approximately sixfold increase in acetylated α-tubulin (Fig. S8), a target of HDAC6 (80). However, other possible mechanisms are beyond the scope of the present study showing that a multitarget approach is a plausible alternative to the one-target–one-disease paradigm in the context of AD.

Finally, pharmacokinetic studies demonstrated that M344 is brain-penetrant, and that our in vivo dosing regimens resulted in sufficiently high CNS concentrations (comparable to the concentrations required to affect gene expression in vitro), but that the drug clears rapidly from plasma and brain. We therefore suggest that drug efficacy relates to C_{max} (discussed above) and that prolonged daily exposure is likely not required. The observations that (*i*) in vivo efficacy was observed with much lower doses of this HDACi than typically used in mouse models of cancer and other CNS disorders (81, 82) and that (*ii*) short periods of high brain exposure seem to be sufficient for efficacy indicate that it may be possible to avoid adverse effects in possible future attempts to use M344 (or related compounds) to treat humans with AD or related disorders.

Conclusion

Using a multifactorial approach to fight a multifactorial disease is necessary. Since the single-target approach has been essentially unsuccessful to date in the treatment of AD, we aimed to use a broader-acting molecule to address the polygenic nature of this disease. In this paper, using an epigenetic approach, we show that it is possible to use one drug compound that simultaneously addresses several aspects of AD, including down- and up-regulation of key AD and neuroprotective genes. We demonstrated that M344, displaying sufficient but transient brain exposure, can prevent memory impairment in the 3xTg (APP_{sw}/$PSEN1_{M146L}$/Tau_{P301L}) AD mouse model. Efficacious in vivo doses of this HDAC inhibitor appear to be much lower than those typically used in animal models for cancer, and brief daily brain exposure seems sufficient. More work is needed with other small-molecule epigenetic compounds to identify the ideal anti-AD profile.

Materials and Methods

Detailed materials and methods are provided in *SI Materials and Methods*. Below are brief descriptions.

Cell Culture. HEK (HEK-293) cells were purchased from ATCC. They were cultured under standard conditions (37 °C, 5% CO_2, 95% air) in Advanced DMEM supplemented with 10% (vol/vol) FBS, penicillin (100 U/mL), streptomycin (100 μg/mL), and Primocin (100 μg/mL). HEK cells overexpressing APP with the Swedish mutation (HEK/APP_{sw}) were a gift from Dennis Selkoe, Brigham and Women's Hospital and Harvard Medical School, Boston, and were cultured in the same media as the HEK-293 cells supplemented with 250 μg/mL of G418 as a selection agent.

NanoString Gene Expression Analysis. For NanoString experiments, cells were treated with either 10 μM of M344 in 0.2% DMSO buffer or 0.2% DMSO buffer alone, in T-75 flasks ($n = 6$). Total RNA was extracted and then used to perform NanoString experiments described in detail by our group (83). The nCounter analysis system (NanoString Technologies) was used to quantify target RNA molecules using these color-coded molecular barcodes. Genes whose fold-change expression was statistically significant and FDR was less than 5% were used for further analysis. A *P* value threshold was set at 0.05.

HDAC Activity Assay. The selectivity profile of M344 was determined biochemically by performing activity assays in duplicate with each of the 11 zinc-dependent HDACs at 10-point 1:3 dilutions, starting at 100 μM (BPS Biosciences). SAHA was used as a positive control for HDACs 1, 2, 3, 6, and 10 since it is known to inhibit those enzymes. TSA was used as a positive control for HDACs 4, 5, 7, 8, 9, and 11 as it has been reported to inhibit these HDACs. All HDAC substrates, buffers, and developers were from BPS BioSciences. Fluorescence signal was measured at 360-nm excitation and 460-nm emission using a Tecan Infinite M1000 microplate reader. Curves were generated with GraphPad Prism 6.0, using a four-parameter nonlinear curve fit to determine the concentration causing IC_{50} values.

ELISAs and Western Blots. $A\beta_{1-40}$ and $A\beta_{1-42}$ were measured from the media and from brain tissue by ELISA with the Novex kit (Life Technologies). An AlphaLISA kit from PerkinElmer was also used to measure $A\beta_{1-42}$ levels in cells. The phosphorylation level of tau at Ser^{396} was measured using an ELISA kit from Thermo Fisher Scientific. All of the kits were used per the manufacturer's instructions. For Western blots, electrophoresed proteins were transferred onto PVDF membranes. All of the primary antibodies were used at 1:1,000 dilution. Membranes were developed using the Clarity ECL detection reagents (Bio-Rad), visualized and then quantified by densitometry, using the Image J software from the NIH.

RT-qPCR. After total RNA extraction, cDNA was synthesized with random hexamers and Moloney Murine Leukemia Virus (M-MLV) reverse transcriptase. Extracted cDNA was used for RT PCR with primers and Taqman Master Mix from Life technologies/Thermo Fisher Scientific. Samples were then amplified for 40 cycles using the Applied Biosystems FAST Real-Time PCR Detection System 7900HT or the Applied Biosystem Quantstudio Flex Real-Time PCR System and analyzed with the SDS Real-Time PCR analysis software (Applied Biosystems). The results presented are based on fold change using the $2^{\wedge-\Delta\Delta Ct}$ method.

Animals and Treatment. We used the triple transgenic (3xTg-AD) mice that overexpress three human transgenes: the APP Swedish double mutation KM670/671NL (APP_{sw}), the presenilin-1_{M146V} mutation ($PS1_{M146V}$), and the Tau_{P301L} mutation (52). Mice were purchased through The Jackson Laboratory, from the NIH-supported Mutant Mouse Regional Resource Center (mmrrc). A cohort of 30 mice was used (50% males and females). Three groups of 10 (5 males and 5 females) were treated intraperitoneally with either vehicle, 3 mg/kg, or 10 mg/kg of M344 diluted in vehicle. An AD prevention paradigm was used where animals were treated from the age of 3 mo, before onset of AD-like pathology. The treatment regimen consisted of 5 d of injection per week for about 4 mo, until animals were killed after behavioral experiments. Behavioral tests were conducted on the mice in the following order: Y-maze spontaneous alternation, open field, novel object recognition, and Barnes maze. For wild-type animal studies, groups of three mice were i.p. treated with 10 mg/kg of M344 at the following time points: 15 min, 30 min, 60 min, 120 min, and 24 h. Brain and plasma were collected as described above and in *SI Materials and Methods*.

All experiments were approved by the University of Miami Miller School of Medicine Institutional Animal Care and Use Committee and conducted according to specifications of the NIH as outlined in the *Guide for the Care and Use of Laboratory Animals* (84).

Brain Distribution and in Vivo Pharmacokinetics. Methods for brain distribution and in vivo pharmacokinetics studies are described in ref. 85.

Statistical Analyses. Unpaired Student's *t* test was used whenever only two means were being compared. One-way ANOVA with either Bonferroni, Dunnett's, or Tukey post hoc analysis was used for multiple comparisons when several means were being compared. Repeated measures two-way ANOVA with Tukey post hoc analysis was used to analyze daily performance.

ACKNOWLEDGMENTS. We thank the members of the Center for Therapeutic Innovation at the University of Miami Miller School of Medicine (UMCTI) for constructive comments throughout this project, and Iris Escobar for help with data collection. This work was mostly funded by Grants 5AZ09 and 6AZ08 (to C.W.) by the Florida Department of Health Ed and Ethel Moore Alzheimer's Disease Research Program. This work was also supported by NIH Grants 4R01DA035055-05 and 5R01AA023781 (to C.W.) and 1R01MH110441 and 1R01NS092671 (to S.P.B.). Seed funds for this project were provided internally from the UMCTI. The NanoString experiments were conducted in the Sylvester Onco-Genomics Shared Resource. ELISAs and RT-qPCR experiments were conducted on equipment from the Sylvester Molecular Therapeutics Shared Resource.

1. Alzheimer's Association (2016) 2016 Alzheimer's disease facts and figures. *Alzheimers Dement* 12:459–509.
2. Saito Y, et al. (2011) Intracellular trafficking of the amyloid β-protein precursor (APP) regulated by novel function of X11-like. *PLoS One* 6:e22108.
3. Tomita S, Kirino Y, Suzuki T (1998) Cleavage of Alzheimer's amyloid precursor protein (APP) by secretases occurs after O-glycosylation of APP in the protein secretory pathway. Identification of intracellular compartments in which APP cleavage occurs without using toxic agents that interfere with protein metabolism. *J Biol Chem* 273: 6277–6284.
4. Hardy J, Selkoe DJ (2002) The amyloid hypothesis of Alzheimer's disease: Progress and problems on the road to therapeutics. *Science* 297:353–356.
5. Mullan M, et al. (1992) A pathogenic mutation for probable Alzheimer's disease in the APP gene at the N-terminus of β-amyloid. *Nat Genet* 1:345–347.
6. Haass C, et al. (1995) The Swedish mutation causes early-onset Alzheimer's disease by β-secretase cleavage within the secretory pathway. *Nat Med* 1:1291–1296.
7. Muratore CR, et al. (2014) The familial Alzheimer's disease APPV717I mutation alters APP processing and Tau expression in iPSC-derived neurons. *Hum Mol Genet* 23: 3523–3536.
8. Hooli B, Tanzi RE (2016) The genetic basis of Alzheimer's disease. *Developing Therapeutics for Alzheimer's Disease: Progress and Challenges*, Wolfe MS, ed (Academic, Boston), pp 23–37.
9. Jonsson T, et al. (2012) A mutation in APP protects against Alzheimer's disease and age-related cognitive decline. *Nature* 488:96–99.
10. Mullard A (2017) BACE inhibitor bust in Alzheimer trial. *Nat Rev Drug Discov* 16:155.
11. Amanatkar HR, Papagiannopoulos B, Grossberg GT (2017) Analysis of recent failures of disease modifying therapies in Alzheimer's disease suggesting a new methodology for future studies. *Expert Rev Neurother* 17:7–16.
12. Extance A (2010) Alzheimer's failure raises questions about disease-modifying strategies. *Nat Rev Drug Discov* 9:749–751.
13. Crump CJ, et al. (2012) BMS-708,163 targets presenilin and lacks notch-sparing activity. *Biochemistry* 51:7209–7211.
14. D'Onofrio G, et al. (2012) Advances in the identification of γ-secretase inhibitors for the treatment of Alzheimer's disease. *Expert Opin Drug Discov* 7:19–37.
15. Swerdlow RH, Burns JM, Khan SM (2010) The Alzheimer's disease mitochondrial cascade hypothesis. *J Alzheimers Dis* 20:S265–S279.
16. Mohandas E, Rajmohan V, Raghunath B (2009) Neurobiology of Alzheimer's disease. *Indian J Psychiatry* 51:55–61.
17. Grundke-Iqbal I, et al. (1986) Microtubule-associated protein tau. A component of Alzheimer paired helical filaments. *J Biol Chem* 261:6084–6089.
18. Brier MR, et al. (2016) Tau and Aβ imaging, CSF measures, and cognition in Alzheimer's disease. *Sci Transl Med* 8:338ra66.
19. de la Torre JC (2010) The vascular hypothesis of Alzheimer's disease: Bench to bedside and beyond. *Neurodegener Dis* 7:116–121.
20. Reitz C, et al.; Alzheimer Disease Genetics Consortium (2013) Variants in the ATP-binding cassette transporter (ABCA7), apolipoprotein E ε4,and the risk of late-onset Alzheimer disease in African Americans. *JAMA* 309:1483–1492.
21. Strittmatter WJ, et al. (1993) Apolipoprotein E: High-avidity binding to beta-amyloid and increased frequency of type 4 allele in late-onset familial Alzheimer disease. *Proc Natl Acad Sci USA* 90:1977–1981.
22. Desikan RS, et al. (2017) Genetic assessment of age-associated Alzheimer disease risk: Development and validation of a polygenic hazard score. *PLoS Med* 14:e1002258.
23. Hollingworth P, et al.; Alzheimer's Disease Neuroimaging Initiative; CHARGE consortium; EADI1 consortium (2011) Common variants at ABCA7, MS4A6A/MS4A4E, EPHA1, CD33 and CD2AP are associated with Alzheimer's disease. *Nat Genet* 43: 429–435.
24. Dulac C (2010) Brain function and chromatin plasticity. *Nature* 465:728–735.
25. Sartor GC, Powell SK, Brothers SP, Wahlestedt C (2015) Epigenetic readers of lysine acetylation regulate cocaine-induced plasticity. *J Neurosci* 35:15062–15072.
26. Volmar C-H, Wahlestedt C (2015) Histone deacetylases (HDACs) and brain function. *Neuroepigenetics* 1:20–27.
27. Magistri M, et al. (2016) The BET-bromodomain inhibitor JQ1 reduces inflammation and tau phosphorylation at Ser396 in the brain of the 3xTg model of Alzheimer's disease. *Curr Alzheimer Res* 13:985–995.
28. Alagiakrishnan K, Gill SS, Fagarasanu A (2012) Genetics and epigenetics of Alzheimer's disease. *Postgrad Med J* 88:522–529.
29. Yu L, et al. (2015) Association of Brain DNA methylation in SORL1, ABCA7, HLA-DRB5, SLC24A4, and BIN1 with pathological diagnosis of Alzheimer disease. *JAMA Neurol* 72:15–24.
30. Bennett DA, et al. (2015) Epigenomics of Alzheimer's disease. *Transl Res* 165:200–220.
31. Gräff J, et al. (2012) An epigenetic blockade of cognitive functions in the neurodegenerating brain. *Nature* 483:222–226.
32. Jung M, et al. (1999) Amide analogues of trichostatin A as inhibitors of histone deacetylase and inducers of terminal cell differentiation. *J Med Chem* 42:4669–4679.
33. Riessland M, Brichta L, Hahnen E, Wirth B (2006) The benzamide M344, a novel histone deacetylase inhibitor, significantly increases SMN2 RNA/protein levels in spinal muscular atrophy cells. *Hum Genet* 120:101–110.
34. Volmar CH, Wahlestedt C, Brothers SP (2017) Orphan diseases: State of the drug discovery art. *Wien Med Wochenschr* 167:197–204.
35. Geiss GK, et al. (2008) Direct multiplexed measurement of gene expression with color-coded probe pairs. *Nat Biotechnol* 26:317–325.
36. Pastori C, et al. (2014) BET bromodomain proteins are required for glioblastoma cell proliferation. *Epigenetics* 9:611–620.
37. Volmar C-H, Ait-Ghezala G, Frieling J, Weeks OI, Mullan MJ (2009) CD40/CD40L interaction induces Abeta production and increases γ-secretase activity independently of tumor necrosis factor receptor associated factor (TRAF) signaling. *Exp Cell Res* 315: 2265–2274.
38. Peng Y, et al. (2006) Effects of huperzine A on amyloid precursor protein processing and β-amyloid generation in human embryonic kidney 293 APP Swedish mutant cells. *J Neurosci Res* 84:903–911.
39. Laporte V, et al. (2008) CD40 ligation mediates plaque-associated tau phosphorylation in β-amyloid overproducing mice. *Brain Res* 1231:132–142.
40. Bakshi P, Margenthaler E, Reed J, Crawford F, Mullan M (2011) Depletion of CXCR2 inhibits γ-secretase activity and amyloid-β production in a murine model of Alzheimer's disease. *Cytokine* 53:163–169.
41. Ait-Ghezala G, et al. (2007) CD40 promotion of amyloid beta production occurs via the NF-kappaB pathway. *Eur J Neurosci* 25:1685–1695.
42. Corder EH, et al. (1993) Gene dose of apolipoprotein E type 4 allele and the risk of Alzheimer's disease in late onset families. *Science* 261:921–923.
43. Calafate S, Flavin W, Verstreken P, Moechars D (2016) Loss of Bin1 promotes the propagation of tau pathology. *Cell Reports* 17:931–940.
44. Ubelmann F, et al. (2017) Bin1 and CD2AP polarise the endocytic generation of beta-amyloid. *EMBO Rep* 18:102–122.
45. Allen M, et al. (2017) ABCA7 loss-of-function variants, expression, and neurologic disease risk. *Neurol Genet* 3:e126.
46. Sakae N, et al. (2016) ABCA7 deficiency accelerates amyloid-β generation and Alzheimer's neuronal pathology. *J Neurosci* 36:3848–3859.
47. Balasubramanyam K, et al. (2004) Polyisoprenylated benzophenone, garcinol, a natural histone acetyltransferase inhibitor, represses chromatin transcription and alters global gene expression. *J Biol Chem* 279:33716–33726.
48. Ando K, Iijima KI, Elliott JI, Kirino Y, Suzuki T (2001) Phosphorylation-dependent regulation of the interaction of amyloid precursor protein with Fe65 affects the production of β-amyloid. *J Biol Chem* 276:40353–40361.
49. Miller CCJ, McLoughlin DM, Lau K-F, Tennant ME, Rogelj B (2006) The X11 proteins, Abeta production and Alzheimer's disease. *Trends Neurosci* 29:280–285.
50. Haass C, Kaether C, Thinakaran G, Sisodia S (2012) Trafficking and proteolytic processing of APP. *Cold Spring Harb Perspect Med* 2:a006270.

51. Lu T, et al. (2014) REST and stress resistance in ageing and Alzheimer's disease. *Nature* 507:448–454.
52. Oddo S, et al. (2003) Triple-transgenic model of Alzheimer's disease with plaques and tangles: Intracellular Abeta and synaptic dysfunction. *Neuron* 39:409–421.
53. Hu C, et al. (2017) Pen-2 and Presenilin are sufficient to catalyze notch processing. *J Alzheimers Dis* 56:1263–1269.
54. Albert JS (2009) 4 - Progress in the development of β-secretase inhibitors for Alzheimer's disease. *Progress Med Chem* 48:133–161.
55. Hu X-T, et al. (2016) Histone deacetylase inhibitor apicidin increases expression of the α-secretase ADAM10 through transcription factor USF1-mediated mechanisms. *FASEB J*, 10.1096/fj.201600961RR.
56. Donmez G, Wang D, Cohen DE, Guarente L (2010) SIRT1 suppresses β-amyloid production by activating the α-secretase gene ADAM10. *Cell* 142:320–332.
57. Malvaez M, et al. (2013) HDAC3-selective inhibitor enhances extinction of cocaine-seeking behavior in a persistent manner. *Proc Natl Acad Sci USA* 110:2647–2652.
58. Koppel I, Timmusk T (2013) Differential regulation of Bdnf expression in cortical neurons by class-selective histone deacetylase inhibitors. *Neuropharmacology* 75:106–115.
59. Sleiman SF, et al. (2016) Exercise promotes the expression of brain derived neurotrophic factor (BDNF) through the action of the ketone body β-hydroxybutyrate. *eLife* 5:e15092.
60. Verghese PB, et al. (2013) ApoE influences amyloid-β (Aβ) clearance despite minimal apoE/Aβ association in physiological conditions. *Proc Natl Acad Sci USA* 110: E1807–E1816.
61. Zhao Z, et al. (2015) Central role for PICALM in amyloid-β blood-brain barrier transcytosis and clearance. *Nat Neurosci* 18:978–987.
62. Ait-ghezala G, et al. (2008) Diagnostic utility of APOE, soluble CD40, CD40L, and Abeta1-40 levels in plasma in Alzheimer's disease. *Cytokine* 44:283–287.
63. Tan J, et al. (1999) Microglial activation resulting from CD40-CD40L interaction after β-amyloid stimulation. *Science* 286:2352–2355.
64. Todd Roach J, et al. (2004) Behavioral effects of CD40-CD40L pathway disruption in aged PSAPP mice. *Brain Res* 1015:161–168.
65. Hanson JE, et al. (2013) SAHA enhances synaptic function and plasticity in vitro but has limited brain availability in vivo and does not impact cognition. *PLoS One* 8:e69964.
66. Benito E, et al. (2015) HDAC inhibitor-dependent transcriptome and memory reinstatement in cognitive decline models. *J Clin Invest* 125:3572–3584.
67. Peleg S, et al. (2010) Altered histone acetylation is associated with age-dependent memory impairment in mice. *Science* 328:753–756.
68. Naert A, et al. (2013) Behavioural alterations relevant to developmental brain disorders in mice with neonatally induced ventral hippocampal lesions. *Brain Res Bull* 94:71–81.
69. Dillon GM, Qu X, Marcus JN, Dodart J-C (2008) Excitotoxic lesions restricted to the dorsal CA1 field of the hippocampus impair spatial memory and extinction learning in C57BL/6 mice. *Neurobiol Learn Mem* 90:426–433.
70. Kilgore M, et al. (2010) Inhibitors of class 1 histone deacetylases reverse contextual memory deficits in a mouse model of Alzheimer's disease. *Neuropsychopharmacology* 35:870–880.
71. Ricobaraza A, et al. (2009) Phenylbutyrate ameliorates cognitive deficit and reduces tau pathology in an Alzheimer's disease mouse model. *Neuropsychopharmacology* 34:1721–1732.
72. Sung YM, et al. (2013) Mercaptoacetamide-based class II HDAC inhibitor lowers Aβ levels and improves learning and memory in a mouse model of Alzheimer's disease. *Exp Neurol* 239:192–201.
73. Gräff J, Tsai L-H (2013) The potential of HDAC inhibitors as cognitive enhancers. *Annu Rev Pharmacol Toxicol* 53:311–330.
74. Cruz JC, et al. (2006) p25/cyclin-dependent kinase 5 induces production and intraneuronal accumulation of amyloid β in vivo. *J Neurosci* 26:10536–10541.
75. Fass DM, et al. (2013) Crebinostat: A novel cognitive enhancer that inhibits histone deacetylase activity and modulates chromatin-mediated neuroplasticity. *Neuropharmacology* 64:81–96.
76. Guan J-S, et al. (2009) HDAC2 negatively regulates memory formation and synaptic plasticity. *Nature* 459:55–60.
77. Rumbaugh G, et al. (2015) Pharmacological selectivity within class i histone deacetylases predicts effects on synaptic function and memory rescue. *Neuropsychopharmacology* 40:2307–2316.
78. Min S-W, et al. (2015) Critical role of acetylation in tau-mediated neurodegeneration and cognitive deficits. *Nat Med* 21:1154–1162.
79. Cohen TJ, et al. (2011) The acetylation of tau inhibits its function and promotes pathological tau aggregation. *Nat Commun* 2:252.
80. Rivieccio MA, et al. (2009) HDAC6 is a target for protection and regeneration following injury in the nervous system. *Proc Natl Acad Sci USA* 106:19599–19604.
81. Hockly E, et al. (2003) Suberoylanilide hydroxamic acid, a histone deacetylase inhibitor, ameliorates motor deficits in a mouse model of Huntington's disease. *Proc Natl Acad Sci USA* 100:2041–2046.
82. Huang H-L, et al. (2015) Novel oral histone deacetylase inhibitor, MPT0E028, displays potent growth-inhibitory activity against human B-cell lymphoma in vitro and in vivo. *Oncotarget* 6:4976–4991.
83. Pastori C, et al. (2015) The Bromodomain protein BRD4 controls HOTAIR, a long noncoding RNA essential for glioblastoma proliferation. *Proc Natl Acad Sci USA* 112:8326–8331.
84. National Research Council (2011) *Guide for the Care and Use of Laboratory Animals* (National Academies Press, Washington, DC), 8th Ed.
85. Young EJ, et al. (2016) Nonmuscle myosin IIB as a therapeutic target for the prevention of relapse to methamphetamine use. *Mol Psychiatry* 21:615–623.
86. Arendash GW, et al. (2001) Progressive, age-related behavioral impairments in transgenic mice carrying both mutant amyloid precursor protein and presenilin-1 transgenes. *Brain Res* 891:42–53.
87. Attar A, et al. (2013) A shortened Barnes maze protocol reveals memory deficits at 4-months of age in the triple-transgenic mouse model of Alzheimer's disease. *PLoS One* 8:e80355.